



CLASSIFICATION OF A FLOOD PROTECTION INFRASTRUCTURE BASED ON ITS VULNERABILITY TO VARIOUS LOADS

Mario Bačić¹, Meho Saša Kovačević¹, Danijela Jurić Kačunić¹, Lovorka Librić¹, Marijan Car¹, Kenneth Gavin², Irina Stipanović³, Cormac Reale⁴

¹ University of Zagreb, Faculty of Civil Engineering, Croatia

² TU Delft, Faculty of Civil Engineering and Geosciences, The Netherlands

³ Infra Plan Consulting doo, Croatia

⁴ University of Bath, Department of Architecture and Civil Eng., United Kingdom

Abstract

The intensity and frequency of flood events is increasing due to climate change impact and accompanying precipitation extremes. However, the impact of a given flood event depends critically on the resilience of the flood defence system, primarily a network of earth embankments and riverbanks. The paper presents the efforts conducted within the ongoing project oVERFLOW, where advanced methodology for vulnerability assessment of critical infrastructure is designed to identify the weakest link in flood protection network. The methodology utilizes the results of advanced asset condition assessment procedures, while sets of relevant loads cover wide range of possible actions for ultimate limit state. As the main output of vulnerability assessment activities, fragility curves are developed. Based on the vulnerability assessment results, the classification and development of inventory of critical infrastructure follows. The validation of methodology is demonstrated on the network of riverbanks and embankments protecting the city of Karlovac from the influence of Kupa river.

Keywords: floods, vulnerability analysis, fragility curve, infrastructure classification

1 Introduction

Flooding events are increasingly occurring worldwide in last several years and as such pose a significant threat to human-life, ecosystems, cultural heritage, and society in general [1]. This owns mostly to the evident climate changes, characterized not necessarily by the increase in precipitation but in the intensity of the precipitation events which heavily affect the earthen structures. Despite all the efforts to predict these events and to increase the resilience of flood protection systems, we are witnessing recent catastrophic floods, such as the 2021 European floods [2] which resulted in 230 fatalities and enormous material damage. During these floods, failure of flood protection systems occurred on several locations, confirming that the resilience of a flood protection system is controlled by the weakest link in the system. This paper presents the efforts of the research project oVERFLOW which deals with vulnerability assessment of embankments and bridges exposed to flooding hazards, with the main objective of identifying the weakest links in flood protection systems. As a basis for this assessment, a worldwide known Dutch flood risk management system VNK2 for embankments [3] is considered, initially developed after disastrous 1953 Great North Sea floods. This system is based on the calculation of the flooding risks based on the probability of failure of flood protection system and on consequences which may arise following the failure.

However, the determination of the probability of failure of a flood protection assets in VNK2 is critically dependent on several highly uncertain parameters. The oVERFLOW project aims to reduce the uncertainties in the VNK2 by using several state-of-the-art non-intrusive and rapid investigation techniques for flood system condition assessment. The results of in-situ investigations feed into the probabilistic models which result in development of so-called fragility curves, eventually providing the classification of the flood protection infrastructure based on its probability of failure for pre-defined loads. The developed methodology is demonstrated on the flood protection system of city of Karlovac.

2 The methodology for flood infrastructure classification based on its vulnerability

The focal point of the methodology is the assessment of flood protection assets through development of fragility curves describing the conditional probability of reaching or exceeding a certain damage state when a hazard of a known intensity occurs [4]. The methodology flowchart is given in Figure 2.

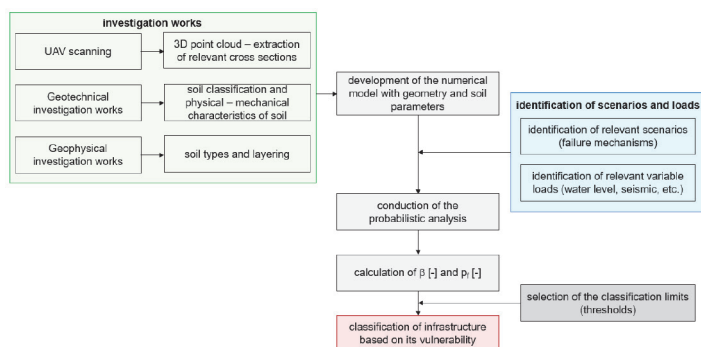


Figure 1 A flowchart of the oVERFLOW methodology for classification of flood protection assets

To collect data on condition of flood protection assets, which will serve as an input for the numerical model, in-situ investigation activities include several methods. Multi-geophysical approach, combining electrical and seismic methods, is accompanied with cone penetration test (CPTU), borehole drillings and laboratory tests, to identify the layering and mechanical characteristics of the assets and subsoil. To obtain data on the terrain topography on a large scale, an Unmanned Aerial Vehicle (UAV) is employed. Besides delivering a highly privileged aerial point of view, which is especially useful along the linear flood protection networks, UAV-based photogrammetry technique results with the generation of 3D georeferenced point cloud, thus providing semi-automatic extraction of terrain cross-sections. The acquired in-situ results feed into numerical probabilistic model. Further, sets of relevant loads on flood protection assets are determined, covering wide range of possible actions for both ultimate and serviceability limit state. In this study, loads include the variation of the water levels and seismic loads, which affect the overall stability of the asset. Even though the scope of the oVERFLOW project includes the analysis of the impact of high-water levels, the objectives were extended with the seismic loads due to very high seismic activity of the case study area in recent period. Two high-magnitude earthquakes hit the case study area in 2020 (M5.5 event with epicentre 60 km NE from Karlovac and M6.2 event with epicentre 50 km SE from Karlovac). These events raised the infrastructure manager's concern of the impact of seismic loads on the riverbanks stability, especially after large-scale failures of the flood protection systems near the epicentre of December 2020 earthquake. As the main output of numerical modelling activities, fragility curves will be developed, and these will be a main

indicator of asset's vulnerability to the pre-defined hazard events. The curves represent the plotted probability of failure vs hazard intensity. In this study, fragility curves are developed through utilization of a limit equilibrium method, where circular sliding surfaces are found for pre-defined number samples of the drained and / or undrained strength parameters, obtained through Monte Carlo sampling technique. From the resulting factor of safety for each sampled strength value, a calculation of reliability index (β) and probability of failure (p_f) follows. These reliability analyses allow for the explicit accounting of uncertainty in both individual properties and geometries, thus providing a probabilistic distribution describing the behaviour of an asset over all possible water level change and seismic loads. The performance function $g(X)$ of an asset is expressed as the difference between the asset's capacity (C) and its demand (D), as reported by [5]:

$$g(X) = (C - D) \begin{cases} > 0, \text{ safe state} \\ = 0, \text{ limit state} \\ < 0, \text{ fail state} \end{cases} \quad (1)$$

where $(X) = g(x_1, x_2, \dots, x_n)$ for $i = 1$ to n . X is a vector containing the different random variables (x_i) required to model the asset's stability level. The reliability index (β) is defined as the number of standard deviations (σ) from the mean (E) of the performance function to the design point:

$$\beta = \frac{E[g(X)]}{\sigma[g(X)]} \quad (2)$$

while the probability of failure (p_f) is defined as the probability at which the performance function is less than zero:

$$P_f = P[g(X) \leq 0] \quad (3)$$

Once the probabilities of failures are calculated for pre-defined loads, an asset classification follows. Within this study, a classification guideline of USACE [6], are considered, Table 1. However, to adapt the classification guidelines to specific problem, each performance level is defined by the range of β (and p_f). Rossi et al. [7] stress out several classification procedures, from which is evident that there is no commonly accepted failure rate in the geotechnical community for slope stability, leading sometimes to significant discrepancies between various studies.

Table 1 Target reliabilities for embankments, modified from the USACE [6]

| Expected performance | Reliability index (β) | Probability of failure (P_f) | Colour coding |
|----------------------|-------------------------------|----------------------------------|---------------|
| High | > 5.0 | < 0.0000003 | 8 |
| | 5.0 to 4.0 | $0.0000003 - 0.000003$ | 7 |
| Good | 4.0 to 3.0 | $0.000003 - 0.001$ | 6 |
| Above average | 3.0 to 2.5 | $0.001 - 0.006$ | 5 |
| Below average | 2.5 to 2.0 | $0.006 - 0.023$ | 4 |
| Poor | 2.0 to 1.5 | $0.023 - 0.07$ | 3 |
| Unsatisfactory | 1.5 to 1.0 | $0.07 - 0.16$ | 2 |
| Hazardous | < 1.0 | > 0.16 | 1 |

3 Implementation of the methodology: flood protection network of Karlovac

3.1 Site overview

The city of Karlovac is situated in the central continental part of Croatia at the intersection of four rivers. As such, it is extremely prone to flooding events where in past many settlements, city districts, local roads and the state road were affected by the high waters. The flood protection system in Karlovac is designed to withstand floods with a 100-year return period, however, the systems has not yet been completed, while several parts of flood protection network are aged and deteriorated. Currently, there are more than 11 km of flood protection systems in the city of Karlovac which are considered as structures of national importance. Within this study, investigated assets include 1.5 km of riverbanks on each side of river Kupa, in the city centre. The riverbanks are up to 10 m high, however with variable geometry and slope angle. At some parts, a stone wall is located on the top of the riverbanks, serving as an additional protection during the high waters.

3.2 Conducted investigation works

An extensive investigation work programme included UAV scanning of the left and right riverbanks, followed by the development of a 3D point clouds, Figure 2, and automatic generation of riverbank cross-sections.



Figure 2 A 3D point cloud of riverbank (left) and geophysical investigations (right)

To determine the riverbank subsoil conditions, as well the variability of key soil parameters for vulnerability analysis, a drilling was performed on five (5) locations, along with soil sampling and laboratory testing. The cone penetration CPTU investigations were conducted on eight (8) locations, evenly distributed along the left and right riverbank of the Kupa. Both drilling and CPTU investigations showed that the soil riverbank soil is mostly formed of fine-grained clayey cover (up to 6 m from terrain surface) overlying the clayey sand material to larger depths. Additionally, the geophysical investigations (Figure 2) of electrical tomography (ERT) and multichannel analysis of surface waves (MASW) were used to supplement the knowledge of geological-structural and physical-mechanical characteristics of the riverbanks. Based on the obtained results, a characteristic geotechnical model of a riverbank is given on Figure 3.

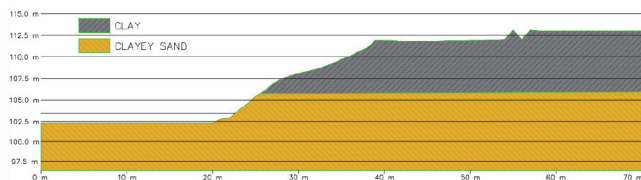


Figure 3 A 3D point cloud of riverbanks and geophysical in-situ investigations

3.3 Probabilistic modelling: development of the fragility curves

Based on the variations in the overall geometry, obtained by UAV scanning, riverbank characteristic zones are identified. Having the results of investigation works in every zone, provided the basis for vulnerability analysis, i.e. development of riverbank fragility curves. The location of each identified zone is shown on Figure 4. The division of riverbank into smaller reaches with sufficiently similar geometry and subsurface conditions enabled their representation by a single two-dimensional model. When the geometrical and layering sources of uncertainties are minimised, the uncertainties are reduced to inherent soil variability of the riverbank and subsoil, and loading conditions [4].

Table 2 gives the overview of the selected parameters used in the probabilistic analysis. While the unit weight is selected as a deterministic (single) value for each layer and derived from the CPT, strength parameters are selected as mean values (μ) along with Coefficient of Variation (CoV) and standard deviation (σ). Also, strength parameters are defined for both drained and undrained condition.

Table 2 Selected values of drained and undrained parameters for numerical analysis

| | Unit wght. [kN/m ³] | Drained parameters | | | | | | Undrained par. | | |
|----|------------------------------------|--------------------|------------|-------------------|--------------------|------------|-----------------|----------------------|------------|-------------------|
| | | Cohesion [kPa] | | | Friction angle [°] | | | Undrained coh. [kPa] | | |
| | | μ [kPa] | CoV [-] | σ [kPa] | μ [°] | CoV [-] | σ [°] | μ [kPa] | CoV [-] | σ [kPa] |
| CL | 18 | 8 | 0,30 | 2,4 | 26 | 0,15 | 3,9 | 35 | 0,30 | 10,5 |
| SC | 19 | 5 | 0,25 | 1,25 | 31 | 0,10 | 3,1 | - | - | - |

To evaluate the vulnerability of the riverbank slopes, global stability is marked as the relevant failure mechanism, where two types of load are analysed: (i) rapid drawdown (RDD), where for each riverbank section, analysis are performed so that water level external to the riverbank slope experiences a rapid reduction in level to a pre - defined level of a low water (106 m a.s.l.), while residual water levels (RWL) in the riverbank remained on higher levels; (ii) seismic stability, where during the increase of the pseudo-static loads the probability of stability failure also increases and where 0.15 g is considered value of peak horizontal acceleration as the value of the 475-year return period in the city of Karlovac. The RDD analyses included drained soil values, while the seismic analyses are performed by using both drained parameters and undrained parameters (for upper clay). Since riverbanks are designed for very rare events with low probability of occurrence, it should be noted that RDD stability and seismic stability analyses are independent. While the seismic analysis is linked to the certain water levels, rapid drawdown scenarios are linked to the ‘after-high-water’ event, since the stability failure occurs after the drawdown of water level external to the slope. Figure 5 shows the resulting fragility curves for one of the riverbanks section on right side (R1) for both RDD and seismic stability.

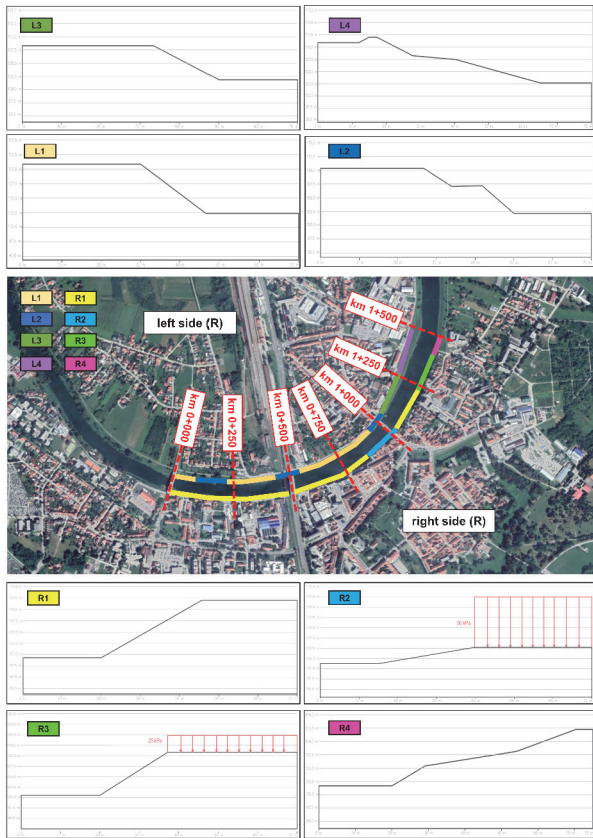


Figure 4 Location of identified riverbank zones based on their geometry

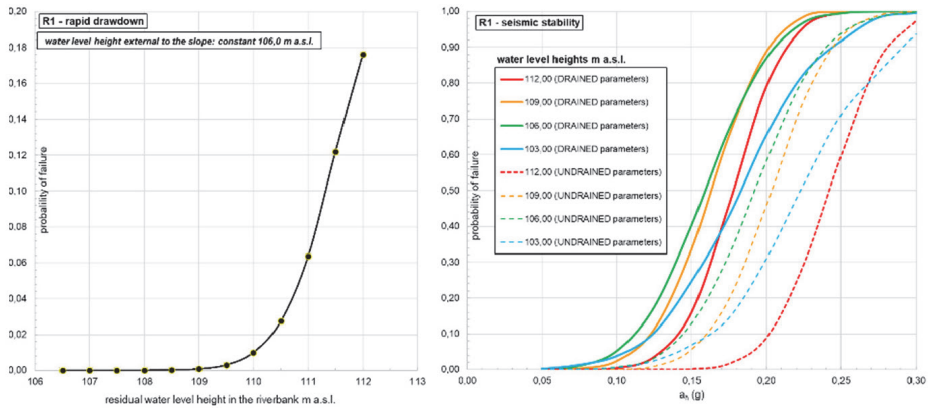


Figure 5 Rapid drawdown (top) and seismic (bottom) fragility curves – zone R1

3.4 Classification of the flood infrastructure

Table 3 show the results of the classification of the analysed section of Karlovac riverbanks for rapid drawdown stability and seismic stability, respectively.

Table 3 Classification of the infrastructure for RDD stability

| Riverbank position: Right side of Kupa river – rapid drawdown | | | | | | | | |
|---|-----------|-------|-----------|-------|-----------|-------|-----------|-------|
| CS Designation | R1 | | R2 | | R3 | | R4 | |
| RWL m a.s.l. | pf (-) | Class |
| 112, 00 | 1, 76E-01 | 1 | 4, 65E-05 | 6 | 5, 33E-01 | 1 | 7, 83E-02 | 2 |
| 111, 00 | 6, 36E-02 | 3 | 4, 65E-05 | 6 | 5, 33E-01 | 1 | 6, 05E-02 | 3 |
| 110, 00 | 9, 97E-03 | 4 | 4, 65E-05 | 6 | 2, 89E-01 | 1 | 3, 77E-02 | 3 |
| 109, 00 | 7, 75E-04 | 6 | 4, 65E-05 | 6 | 6, 54E-02 | 3 | 1, 57E-02 | 4 |
| 108, 00 | 5, 03E-05 | 6 | 4, 65E-05 | 6 | 7, 47E-03 | 4 | 4, 05E-03 | 5 |
| 107, 00 | 2, 12E-05 | 7 | 4, 65E-05 | 6 | 6, 83E-04 | 6 | 1, 54E-03 | 5 |
| Riverbank position: Left side of Kupa river – rapid drawdown | | | | | | | | |
| CS Designation | L1 | | L2 | | L3 | | L4 | |
| RWL m a.s.l. | pf (-) | Class |
| 112, 00 | 2, 39E-01 | 1 | 3, 01E-07 | 7 | 1, 93E-03 | 5 | 7, 55E-03 | 4 |
| 111, 00 | 2, 39E-01 | 1 | 3, 01E-07 | 7 | 1, 93E-03 | 5 | 2, 76E-03 | 5 |
| 110, 00 | 1, 01E-01 | 2 | 2, 60E-07 | 8 | 1, 93E-03 | 5 | 3, 98E-04 | 6 |
| 109, 00 | 1, 29E-02 | 4 | 2, 13E-07 | 8 | 1, 93E-03 | 5 | 1, 40E-05 | 7 |
| 108, 00 | 4, 38E-04 | 6 | 1, 51E-07 | 8 | 1, 20E-03 | 5 | 5, 51E-08 | 8 |
| 107, 00 | 1, 17E-05 | 7 | 4, 99E-08 | 8 | 2, 43E-04 | 6 | 1, 57E-07 | 8 |
| Riverbank position: Right side of Kupa river – 0.15 g seismic loading | | | | | | | | |
| CS Designation | R1 | | R2 | | R3 | | R4 | |
| WL m a.s.l. | pf (-) | Class |
| 112, 00 | 1, 60E-01 | 2 | 1, 00E-04 | 6 | 4, 40E-01 | 1 | 1, 60E-05 | 7 |
| 109, 00 | 3, 50E-01 | 1 | 1, 00E-04 | 6 | 7, 40E-01 | 1 | 1, 00E-01 | 2 |
| 106, 00 | 4, 10E-01 | 1 | 1, 00E-04 | 6 | 7, 10E-01 | 1 | 1, 40E-01 | 2 |
| 103, 00 | 2, 50E-01 | 1 | 3, 00E-04 | 6 | 4, 60E-01 | 1 | 1, 40E-01 | 2 |
| Riverbank position: Left side of Kupa river – 0.15 g seismic loading | | | | | | | | |
| CS Designation | L1 | | L2 | | L3 | | L4 | |
| WL m a.s.l. | pf (-) | Class |
| 112, 00 | 2, 00E-02 | 4 | 2, 00E-02 | 4 | 2, 80E-04 | 6 | 1, 64E-05 | 7 |
| 109, 00 | 9, 00E-02 | 2 | 4, 10E-03 | 5 | 2, 80E-04 | 6 | 1, 06E-01 | 2 |
| 106, 00 | 7, 00E-02 | 2 | 5, 00E-02 | 3 | 9, 80E-04 | 6 | 1, 35E-01 | 2 |
| 103, 00 | 7, 50E-03 | 4 | 2, 00E-02 | 4 | 6, 30E-05 | 6 | 1, 36E-01 | 2 |

Here, a slope geometry has crucial role in the stability, where cross-sections R1 and L1 are characterized by steepest slopes, see Figure 4, and thus highest probability of failure. Also, cross-section R3 yielded high probability of failures mostly due to additional load of buildings resting atop of riverbank at this location.

4 Conclusions

To conduct the classification of a flood protection infrastructure based on their vulnerability to various loads, as foreseen by the proposed methodology, information on a geometry and subsoil variations could be obtained by efficient, yet rapid and inexpensive methods, whose results serve as the input for probabilistic numerical models. A demonstration of the methodology is shown on the example of Karlovac city riverbanks, which are divided into smaller reaches with sufficiently similar geometry and subsurface conditions. Calculation of the probability of failure of a given section of a riverbank enabled classification of the assets based on the probability of failure for various water levels and seismic loads. Even though the methodology is developed for flood protection network, it could be easily adapted for transportation network, also characterized by a linear nature.

Acknowledgments

This research was funded by EU Civil Protection Mechanism, GA 874421: oVERFLOW (Vulnerability assessment of embankments and bridges exposed to flooding hazard).

References

- [1] Bačić, M., Kovačević, M.S., Librić, L., Perić, T.: Impact of climate changes on the flood protection system: example of the oVERFLOW project, Proceedings of the 8th congress of Croatian Builders, pp. 517-526, Vodice, Croatia, 3. – 5. October 2021, DOI:10.14256/8SHG.2021.156
- [2] Fekete, A., Sandholz, S.: Here Comes the Flood, but Not Failure? Lessons to Learn after the Heavy Rain and Pluvial Floods in Germany 2021, *Water*, 13 (2021), 3016, DOI: <https://doi.org/10.3390/w13213016>
- [3] VNK2 project office Flood Risk in the Netherlands, VNK2: The Method in Brief, 2012
- [4] Rossi, N., Bačić, M., Kovačević, M.S.: Evaluation of seismic resilience of levees through the development of fragility curves, Proceedings of the 1st Croatian Conference on Earthquake Engineering - 1CroCEE, pp. 373-383, Zagreb, Croatia, 22. – 24. March 2021, DOI: 10.5592/CO/1CroCEE.2021.273
- [5] Kovačević, M.S., Bačić, M., Gavin, K.: Application of neural networks for the reliability design of a tunnel in karst rock mass, *Canadian Geotechnical Journal*, 58 (2021) 4, pp. 455–467, DOI: 10.1139/cgj-2019-0693
- [6] USACE Introduction to Probability and Reliability Methods for Use in Geotechnical Engineering, Engineering and Design, Washington, D.C., 1997
- [7] Rossi, N., Bačić, M., Kovačević, M.S., Librić, L.: Development of Fragility Curves for Piping and Slope Stability of River Levees, *Water*, 13 (2021) 5, 738, DOI: 10.3390/w13050738